NASA TECHNICAL MEMORANDUM

NASA TM X- 67966

NASA TM X- 67966

DYNAMICS OF HEAT-PIPE REACTORS

by George F. Niederauer
Lewis Research Center
Cleveland, Ohio

TECHNICAL PAPER presented at
Winter Meeting of the American Nuclear Society
Miami, Florida, October 17-21, 1971

E-6678

DYNAMICS OF HEAT-PIPE REACTORS

by

George F. Niederauer

Lewis Research Center

ABSTRACT

A split-core heat-pipe reactor fueled with either 233-UC or 235-UC in a tungsten cermet and cooled by 7-Li-W heat pipes is examined for the effects of the heat pipes on this reactor in trying to safely absorb large reactivity inputs through inherent shutdown mechanisms. Limits on ramp reactivity inputs due to fuel-melting temperature and heat-pipe wall heat flux are mapped for the reactor in both startup and at-power operating modes.

DYNAMICS OF HEAT-PIPE REACTORS

BY

George F. Niederauer

Lewis Research Center

INTRODUCTION

An introduction to the concept of split-core heat-pipe reactors is presented in another paper at this conference (1). In that paper it was shown that heat pipes can have a great effect on the design of a reactor. It is the intention of this paper to examine some of the effects of heat pipes on reactor dynamics, especially from a viewpoint of inherent safety.

HEAT PIPES

The use of heat pipes for heat removal represents a significant departure from conventional schemes of heat removal. By using heat pipes each coolant channel is replaced with an independent, sealed coolant loop which is self-starting and self-regulating, using only a fraction of the coolant required in equivalent conventional liquid-cooled loops.

Heat pipe reactors have different coolant phenomena to examine. In a conventional liquid metal reactor, heat is transferred by convection from the fuel to the coolant and passed out of the reactor as part of the thermal capacity of the fluid. The coolant flow rate is adjusted and controlled independently of the heat flux rate into the coolant. In a heat pipe reactor (fig. 1) the reactor heat is conducted through the heat pipe wall to the coolant, but the coolant flow rate is coupled to the heat flux rate. (The coolant is normally in a liquid state, but in certain cases may be solid during the initial startup of a reactor.) The heat transferred to the heat pipe causes the coolant inside the heat pipe to evaporate and flow out of the reactor. The coolant is then condensed back to the liquid state in the "condenser" part of the heat pipe. The liquid then flows by capillary action through the wick back to the evaporator. The near-equilibrium conditions of the liquid and vapor phases in the heat pipe at steady state result in a small ΔT (usually just a few degrees) along the length of the pipe. Although a heat pipe transfers heat in the forms of kinetic energy and heat capacitance, these are negligible in comparison to that transferred in the heat of vaporization of the coolant.

There are two types of heat pipe operations under study: startup and at-power. During startup the coolant vaporizes in the evaporator and builds up pressure in this region. A pressure front forms across the pipe at the condenser end of the evaporator section. In this pressure front the vapor is condensed into the coolant contained in the wick and coolant channels, thereby giving up its heat of vaporization. In these studies the speed at which the front moves down the pipe is assumed to be controlled by the rate at which the coolant and wick are brought up to the evaporator temperature. This is a conservative approach in that the front is assumed to be moving more slowly than it might in an actual heat pipe. In reality, the front may move down the pipe while bringing the coolant only partway up to the evaporator temperature.

With both reactor and heat pipe in a normal operation mode at power, the transport of energy by vapor flow from the evaportor to the condenser, as in startup, is significant only by heat of vaporization. Also, the heat capacity in the vapor is negligible compared with the liquid. Hence, the thermal resistance added by the vapor region may be considered nil, and the net thermal resistance in the heat pipe is effectively due to that for the radial heat conductance in the walls and liquid coolant regions only. Thus, a heat pipe with an average distance between evaporator and condenser of 18 cm has an effective thermal resistance length of only 0.3 cm.

NODAL MODEL

A nodal model for use in computer calculations is shown in figure 2. It is a non-scale representation of an average fuel piece and heat pipe, along with an appropriate part of the center plate and radial reflector. A radiator heat pipe is added to act as a heat sink in the at-power studies. It is sized for the reactor operating at 1 MW thermal and takes the place of the long heat pipes and the rest of the thermionic conversion system discussed in reference 1 but which are not significant for these studies.

Note that the heat pipe lacks vapor nodes and that it has three axial nodes, one evaporator and two condenser nodes. In at-power studies the middle heat pipe node acts more like an adiabatic region since much more heat is dumped through the heat exchanger; however, it is important in heating up the axial reflector during transients. In startup studies the middle nodes are the only condenser nodes until this region is heated up to the evaporator temperature. Then the pressure front moves from the middle region into the heat exchanger region. For the purposes of these studies it is assumed that in the important part of the startup transients the reactor heat pipe has not completed the startup phase; that is, the end condenser nodes and the radiator heat pipe nodes are absent, and the pressure moves from the remaining condenser section to outside that section during the startup transients.

Doppler effects are deemed important for those materials located within the core boundaries. These materials are the tungsten in the wick, heat pipe wall, fuel cermet and center plate, and the uranium in the fuel. Their reactivity coefficients are nonlinear; the tungsten effect varies as $T^{-0.8}$ and uranium, as T^{-1}.

Expansion effects include those regions located within the reflector boundaries, that is, fuel, center structure, axial and radial reflectors, heat pipe walls. The fuel is assumed mated to the heat pipes, thus, the axial fuel expansion effect is located in the heat pipe wall. The core is constrained radially by the radial reflector, hence, the radial fuel expansion effect is in the radial reflector. The expansion reactivity effects are all considered to be linear functions of temperature.

All of the Doppler and expansion effects have negative reactivity coefficients except the fuel Doppler coefficient, and its value is several times greater than the cermet tungsten Doppler coefficient; however, the negative fuel expansion coefficient by itself is an order of magnitude greater than the positive fuel Doppler coefficient, as shown in table 1. It is mainly the speed at which the delayed effect of the larger fuel expansion coefficient can be realized to overcome the prompt effect of the fuel Doppler coefficient that sets the limits for safe inherent shutdown of this reactor following a positive external reactivity insertion.

To perform these studies the reactor dynamics code AIROS (6) has been modified to handle nonlinear reactivity coefficients, heat transfer from radiators, heat pipe startup, and stepping of the startup front down a nodal model of the heat pipe. The unsteady heat balance in the coolant in the hot zone during startup is

$$mC_p \frac{dT_L}{dt} = (uA)_{WL} (T_W - T_L) - \omega h \tag{1}$$

where ω is the heat flux out of the hot zone and the other terms have conventional meanings (subscripts W and L indicate heat pipe wall and liquid coolant). The vapor mass flow rate is (7)

$$\omega = AB\left[\frac{k}{2(k+1)RT_L}\right]^{1/2} \exp\left[-h/RT_L\right] \qquad (2)$$

where

A = vapor flow cross-sectional area
B = vapor constant = p exp (h/RT)
k = Cp/Cv = 5/3
R = gas constant
h = heat of vaporization

TYPICAL TRANSIENTS

Typical characteristics of startup transients are shown through the illustration of a single transient in figure 3; this is for a reactivity ramp input at a 10¢/sec rate to an 80¢ level in both a 233-UC and a 235-UC reactor. Starting with 1 n/cm^3 neutron densities and just-critical reactors we find the fuel temperatures rising from 300K to 1173K in 233-UC reactor and 1728K in the 235-UC reactor. A more dramatic comparison is made between the heat fluxes through the heat pipe walls: a peak of 14.5 watts/cm^3 for 233-UC compared to 282 for 235-UC. This difference is not so wide in slower ramps.

Typical characteristics of at-power transients are shown in figure 4, also for 10¢/sec ramps to 80¢ levels. In this case we start with critical reaction operating at 1 MW thermal. The temperature rises are not as pronounced as in the startup cases, but the peaks are higher: 2490K for 233-UC and 3697 for 235-UC. The latter peak is above the melting temperature of UC; hence, a given ramp will give rise to a less safe transient in an at-power situation than in a reactor startup. Note also that both reactors display high heat pipe wall heat fluxes of the same order of magnitude.

PARAMETRIC ANALYSIS

Taking just the peaks of the fuel temperatures and the heat pipe wall heat fluxes from many cases where only the reactivity ramp rate and level have been varied results in figure 5 for reactor startup and in figure 6 for the reactors at power. In figure 5 we find that ramps of lower levels and higher rates, including all levels for rates above a point called the critical ramp rate, behave as step reactivity inputs, i.e., they are independent of the rate. The critical ramp rate is defined as the rate above which the reactor cannot shut down inherently from reactivity insertions of more than 1\$. In the startup situation we find that the critical ramp rate is about 6¢/sec for the 233-UC reactors and about double this for the 235-UC reactors. The melting temperatures for UC so far reported (7) cover the shaded band between 2550K and 2860K. Below the critical ramp rate large reactivity insertions can be handled safely by these reactors, but above this rate the insertions must be kept at least several cents below a dollar.

Besides the melting point of the fuel another limiting factor is reactor operation in heat pipe burnout. One measure of this is the maximum radial heat flux which can be taken by the heat pipe without causing burnout, which may occur by vaporizing the liquid coolant faster than the capillary pump can return it. These limits will depend upon the quality and engineering of the heat pipes and will need to be tested experimentally. Experiments have shown that Li-W heat pipes are capable of at least 300 watts/cm^2 continuous operation. The limits of continuous operation have not yet been reached but Loewe (8) has stated that they could be as high as 1000 watts/cm^2. It may be possible that higher fluxes can be taken for a short time, but this has yet to be proven. Until more experiments can answer these problems more confidently, a 300 watts/cm^2 limit will be considered a conservative limit for operation. It is shown in figure 5 that this leads to a greater restriction than does the fuel melting temperature, but one that shows promise of being lifted.

The results for at-power transients, plotted in the same manner as in figure 5, are shown in figure 6. The critical ramp rates still exists, but they are now reached only by ramp inputs with levels higher than those which cause fuel melting, so they are not a problem here. As noted in the discussion of some typical transients, the at-power reactor is more sensitive to the reactivity input level. In the range of interest, i.e., where peak fuel temperatures are below the melting point, ramps greater than 20¢/sec for 233-UC and 3¢/sec for 235-UC behave as step inputs. The limits imposed by fuel melting are 87¢ for 233-UC and 35¢ for 235-UC. In the case of the 233-UC reactor this restriction is further tightened if a 300 watt/cm^2 heat flux limit were to be imposed.

CONCLUSION

Three basic results have been achieved in this analysis of heat pipe reactor dynamics. First: these reactors can safely handle insertions of more than a dollar's worth of reactivity if it is done slowly enough for the inherent shutdown mechanisms to handle it. Second: operation of these reactors at-power is more limited than during startup. Third: a 233-UC-fueled split-core heat-pipe reactor can take more reactivity in terms of dollars than can the 235-UC-fueled reactors. Finally, in performing this analysis we have begun the development of a computer code for the investigation of heat pipe reactor dynamics.

REFERENCES

1. G. F. NIEDERAUER, E. LANTZ, and R. BREITWIESER, "Split-Core Heat-Pipe Reactors for Out-of-Pile Thermionic Power Systems," Am. Nucl. Soc. Trans., 14, 433 (1971).

2. R. L. BREHM, "Estimate of Doppler Coefficients for In-Pile Thermionic Reactor Materials," JPL-TR-32-1077, Jet Propulsion Lab., California Institute of Technology (October 1, 1967).

3. M. R. HACKNEY and S. C. COHEN, "Neutronic Comparison of Low-Power Thermionic Reactors," 1969 Thermionic Conversion Specialists Conference, Carmel, California (October 21-23, 1969).

4. R. E. SHAVER and N. G. WITTENBROCK, "Review of Reactor Safety Analysis of Fast and Liquid Metal Cooled Reactors," BNWL-477, Battelle Northwest (November 1967).

5. G. F. NIEDERAUER and E. LANTZ, "A Split-Core, Heat-Pipe Reactor for Space Power Applications," 1970 Thermionic Conversion Specialist Conference, Miami Beach, Florida (October 26-29, 1970).

6. R. A. BLAINE and R. F. BERLAND, "AIROS: A Digital Simulator for Power Reactor Dynamics," NAA-SR-9943, Atomics International (August 1, 1964).

7. G. F. BURDI, ed., "SNAP Technology Handbook, Vol. III, Refractory Fuels and Claddings," NAA-SR-8617, Atomics International (April 30, 1965).

8. W. G. LOEWE, "Out-of-Core Thermionic Space Power," Second Intern. Conf. Thermionic Electric Power Generation, Stresa, Italy (May 1968).

TABLE 1. REACTIVITY COEFFICIENTS

	^{233}U		^{235}U	
	$10^{-6}\ \frac{\delta k/k}{K}$	$10^{-4}\ \frac{\$}{K}$	$10^{-6}\ \frac{\delta k/k}{K}$	$10^{-4}\ \frac{\$}{K}$
EXPANSION				
Axial Fuel	-3.20	-11.19	-3.02	-4.51
Radial Fuel	-5.24	-18.30	-2.01	-3.00
Axial Reflector	-1.26	-4.41	-0.89	-1.33
Radial Reflector	-8.24	-28.81	-7.25	-10.82
Center Structure	-0.26	-0.91	-0.18	-0.26
Heat Pipe	-0.18	-0.61	-0.12	-0.18
DOPPLER				
Fuel	0.33	1.14	0.11	0.16
Cermet Tungsten	-0.06	-0.20	-0.06	-0.09
Heat Pipe	-0.20	-0.70	-0.11	-0.17
Center Structure	-0.04	-0.13	-0.03	-0.05

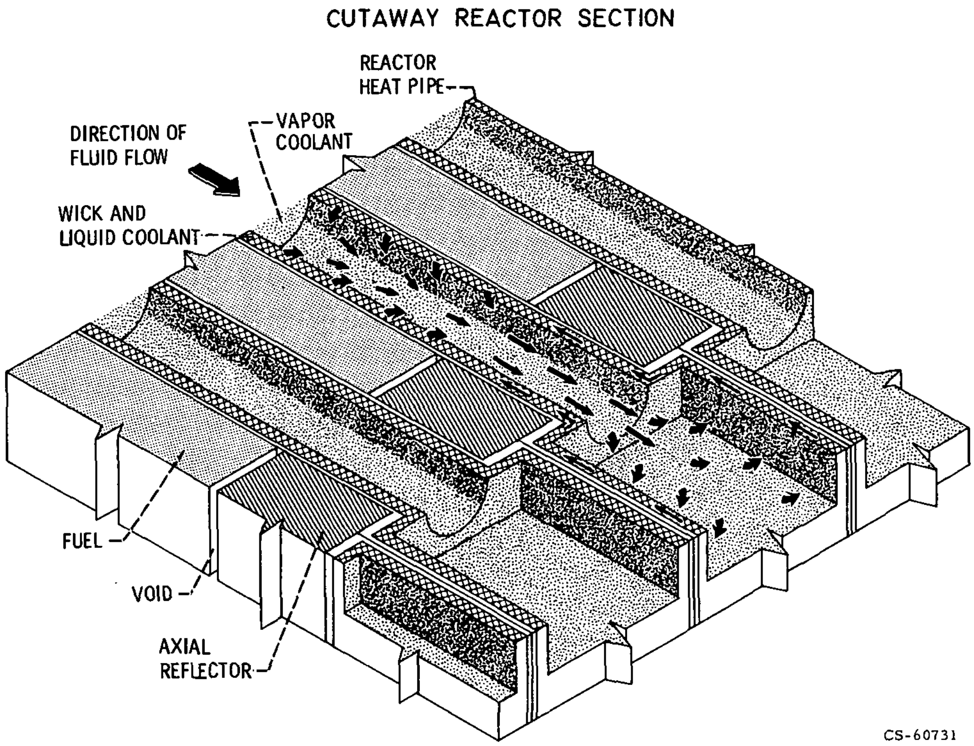

Figure 1. - Cutaway reactor section.

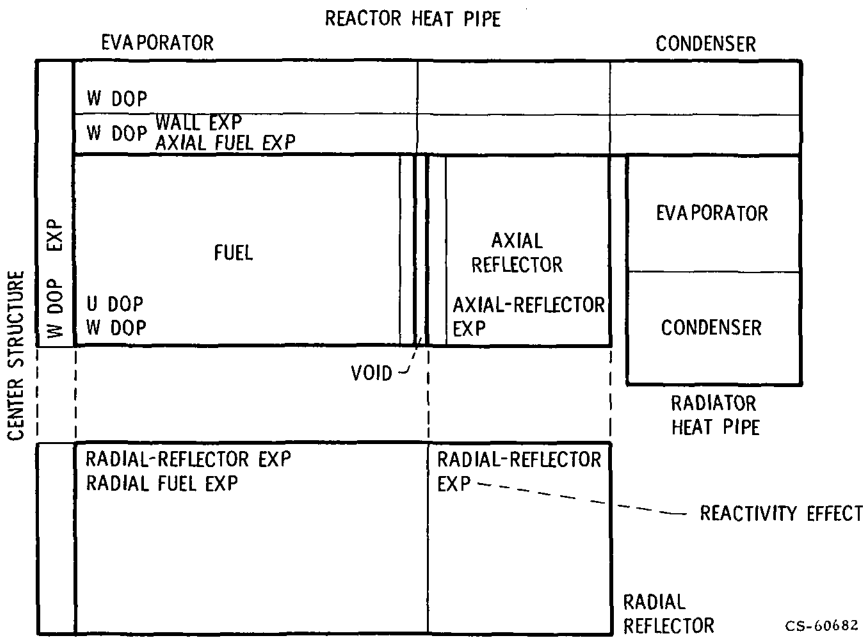

Figure 2. - Nodal model.

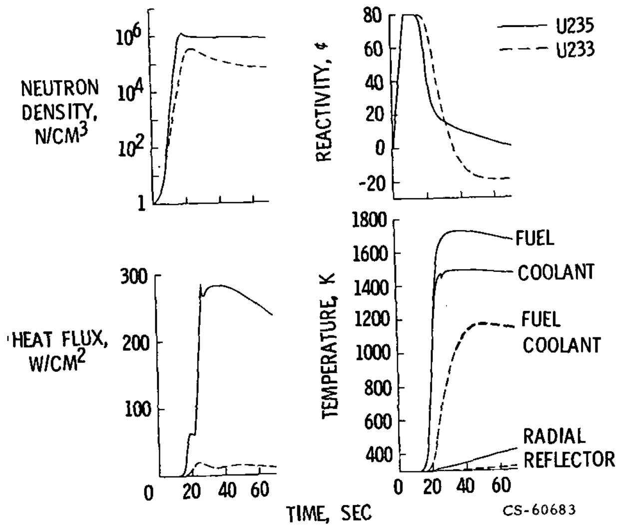

Figure 3. - Startup transient - 10¢/sec to 80¢.

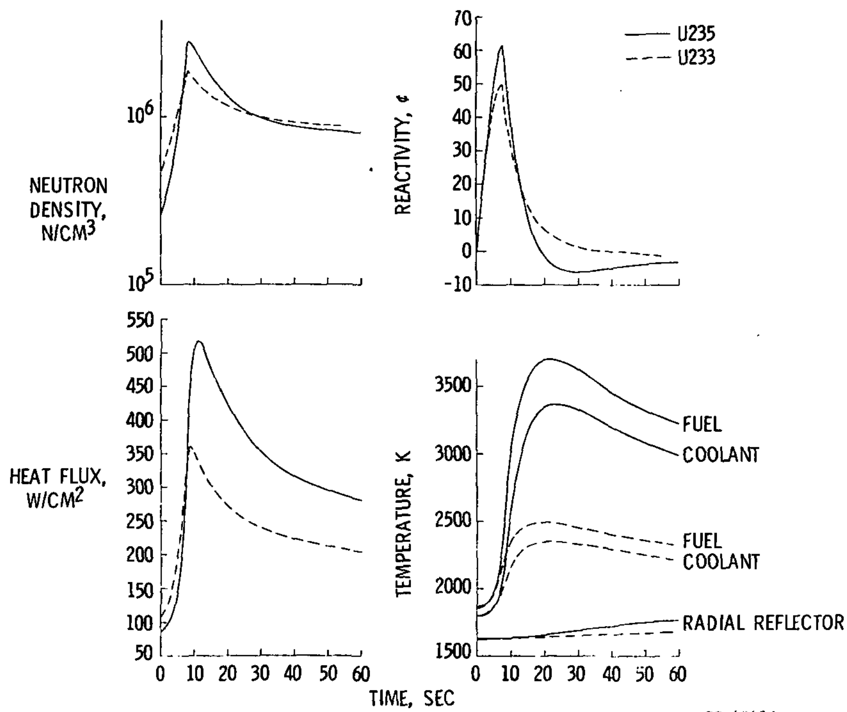

Figure 4. - At-power transient 10¢/sec to 80¢.

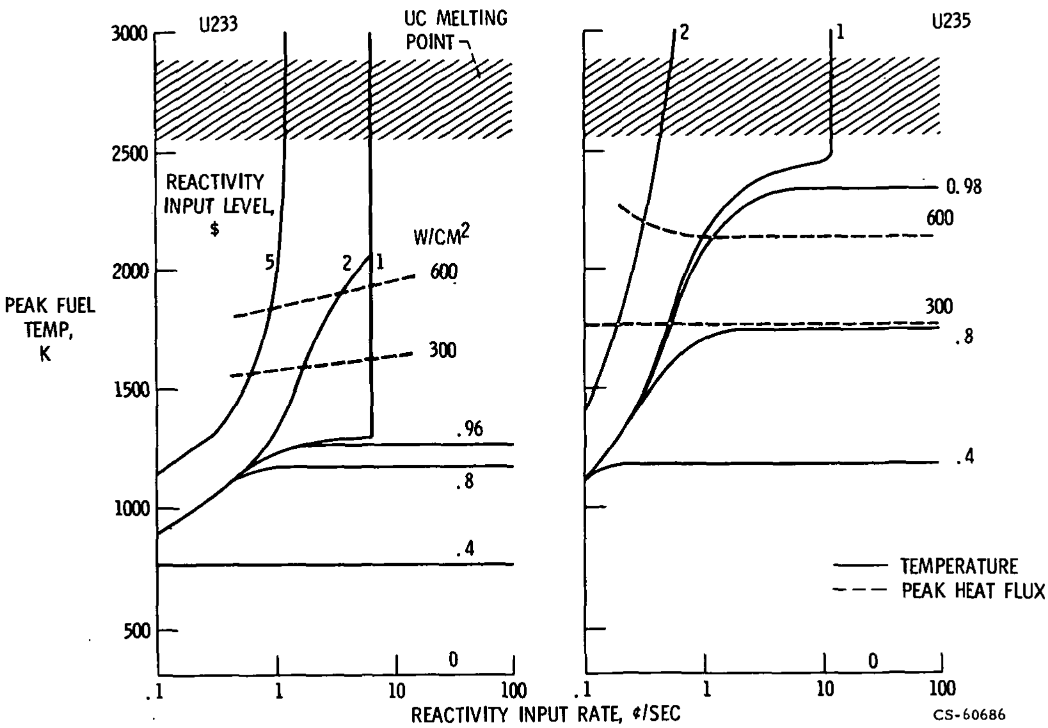

Figure 5. - Peak fuel temperatures for startup.

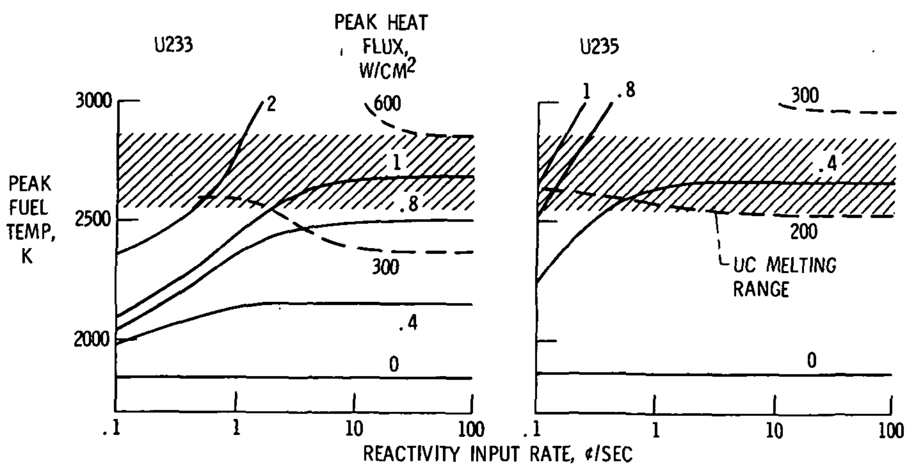

Figure 6. - Peak fuel temperatures at power.